

adults consume a diet where fructose is the sole source of carbohydrates until tolerance can be evaluated.

References

1. Thiagarajah JR, Kamin DS, Acra S, Goldsmith JD, Roland JT, Lencer WI, et al. Advances in evaluation of chronic diarrhea in infants. *Gastroenterology*. 2018;154, 2045–2059.e6.
2. Lindquist.F B, Meeuwisse.F G.W. Chronic diarrhoea caused by monosaccharide malabsorption. *Acta Paediatr*. 1962;51:674–85.
3. Martín MG, Turk E, Lostao MP, Kerner C, Wright EM. Defects in Na⁺/glucose cotransporter (SGLT1) trafficking and function cause glucose–galactose malabsorption. *Nat Genet*. 1996;12: 216–20.
4. Abad-Sinden A, Borowitz S, Meyers R, Sutphen J. Nutrition management of congenital glucose–galactose malabsorption: a case study. *J Am Diet Assoc*. 1997;97:1417–21.
5. Stenson PD, Ball EV, Mort M, Phillips AD, Shiel JA, Thomas NST, et al. Human gene mutation database (HGMD): 2003 update. *Hum Mutat*. 2003;21:577–81.
6. Xin B, Wang H. Multiple sequence variations in SLC5A1 gene are associated with glucose–galactose malabsorption in a large cohort of Old Order Amish. *Clin Genet*. 2011;79:86–91.

Blanca Lodoso-Torrecilla^a, Guiomar Perez de Nanclares^{b,*}, Intza Garin^c, Ariane Calvo-Saez^d, Idoia Martinez-Fernandez de Pinedo^a

^a Grupo de Investigación en Enfermedades Raras, Unidad Neonatal, Servicio de Pediatría, Instituto de Investigación Sanitaria BioAraba, OSI Araba, Vitoria-Gasteiz, Spain

^b Grupo de Investigación de Enfermedades Raras, Laboratorio de (Epi)Genética Molecular, Instituto de Investigación Sanitaria BioAraba, OSI Araba-Txagorritxu, Vitoria-Gasteiz, Spain

^c Laboratorio de Genética, UGC Laboratorio, OSI Araba, Vitoria-Gasteiz, Spain

^d Sección de Gastroenterología, Hepatología y Nutrición Pediátrica, OSI Araba, Vitoria-Gasteiz, Spain

*Corresponding author.

E-mail address: gnanclares@osakidetza.eus

(G. Perez de Nanclares).

2341-2879/ © 2019 Published by Elsevier España, S.L.U. on behalf of Asociación Española de Pediatría. This is an open access article under the CC BY-NC-ND license (<http://creativecommons.org/licenses/by-nc-nd/4.0/>).

Advances in the diagnosis of ocular toxoplasmosis: Use of optical coherence tomography[☆]



Novedades para el diagnóstico de la toxoplasmosis ocular: uso de la tomografía de coherencia óptica

Dear Editor:

Ocular toxoplasmosis (OT) is the leading cause of posterior uveitis in immunocompetent patients. The primary infection is asymptomatic in most cases, and therefore OT is commonly diagnosed in subsequent reactivations manifesting with characteristic chorioretinal scars (white-yellow lesions with greyish edges, usually unilateral).

From a clinical standpoint, paediatric patients may present with retinochoroiditis and be asymptomatic, with blurry vision due to vitreitis or with bloodshot eyes and ocular pain, frequently associated with anterior uveitis. The pathogenesis of such reactivations remains unclear.¹

The diagnosis is made based on the described clinical manifestations combined with compatible serological findings. Most patients have low IgG titres and negative IgM titres, so IgG avidity or increased titres may be useful for diagnosis.² Challenging cases may require the use of invasive techniques, such as polymerase chain reaction (PCR)

analysis for detection of *Toxoplasma gondii* in aqueous or vitreous humour³; however, this is considered an aggressive technique.

We present 3 cases of acquired OT in paediatric patients, describing characteristic signs that can be assessed by optical coherence tomography (OCT) and that contributed to the early and accurate diagnosis of the disease.

Case 1: girl aged 8 years from Equatorial Guinea that presented with acute unilateral anterior uveitis manifesting with eye pain and redness. The patient underwent immunological testing and screening for infections including serological tests for antibodies against *Toxoplasma*, with a negative result for IgM antibodies and a positive result for IgG antibodies. The fundus appeared normal in the initial examination. In subsequent evaluations, the patient had elevation of IgG antibodies and the OCT revealed retinitis with stalagmite-like raised lesions in the inner perimacular surface, suggestive of toxoplasmosis⁴ (Fig. 1).

Case 2: boy age 12 years of Spanish descent presenting with headache and loss of visual acuity (0.8). Examination of the fundus revealed focal chorioretinitis focal with vitreitis, compatible with toxoplasmosis, while serological testing for antibodies against *Toxoplasma* was negative for IgM and positive for IgG. Subsequent evaluations revealed a 4-fold increase in IgG titres. Treatment started with antibiotherapy and systemic steroid therapy. The outcome was parafoveal scarring with absence of photoreceptors and small retinal cysts, with normal visual acuity (Fig. 2).

Case 3: girl aged 10 years of Moroccan descent presenting with panuveitis with acute granulomatous anterior uveitis in the left eye. The ophthalmological evaluation by means of OCT revealed areas of inflammation, signs of vitreitis and inflammation of the inner layers of the retina. Ocular toxoplasmosis was suspected, leading to serological testing, which was positive for IgG, with a titre of more

[☆] Please cite this article as: Ferrer Mellor T, et al. Novedades para el diagnóstico de la toxoplasmosis ocular: uso de la tomografía de coherencia óptica. *An Pediatr (Barc)*. 2020;92:105–106.

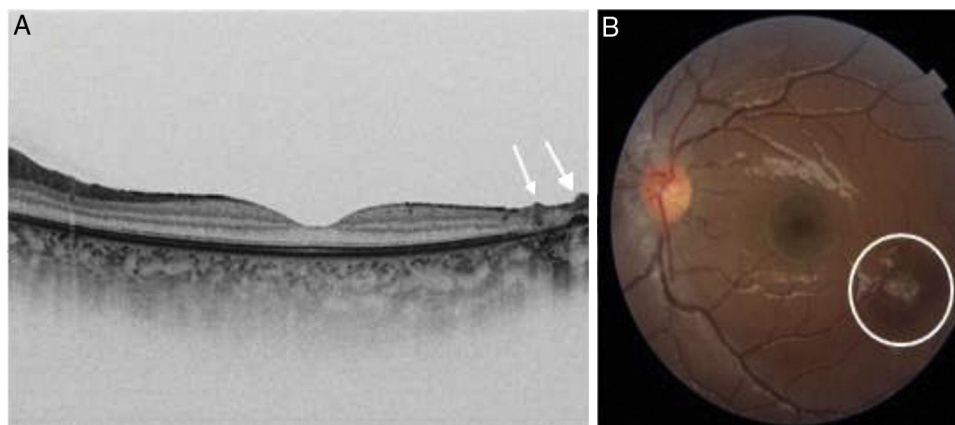


Figure 1 A) Image obtained by OCT showing hypertrophy of the retinal pigment epithelium and absence of the retinal layered structure. Hyperreflective staghmite-like preretinal deposits (arrow). B) Photograph of the eye fundus showing a typical chorioretinal scar (circle).

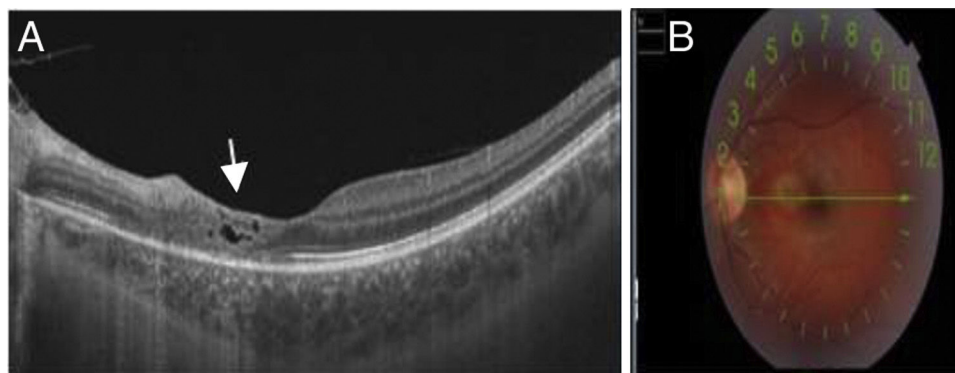


Figure 2 A) OCT image. Cystic spaces in the inner layer of the retina. Cystic spaces are a frequent finding in patients with toxoplasmosis and considered a complication (parasite-filled cysts or signs of local inflammation or exudates). B) Photograph of the eye fundus showing the paramacular chorioretinal scar in the nasal fundus, consistent with the OCT findings.

than 200 U/mL, and negative for IgM. The patient started a course of antibiotherapy, to which she responded favourably. Subsequent ophthalmologic evaluations revealed an area of chorioretinal atrophy with absence of pigmentation in the margins. Visual acuity was not affected.

These 3 patients were treated with pyrimethamine-sulfadiazine and oral corticosteroids, to which they responded favourably. The clinical and serological outcomes confirmed the diagnosis of uveitis secondary to *Toxoplasma* infection. In OCT, focal retinitis with adjacent vitreitis is highly suggestive of OT. Newly identified clinical signs that may be found with OCT, such as early signs of inflammation (staghmite-like lesions) (Fig. 1), or residual signs, such as retinal cysts⁵ (Fig. 2) are not specific for toxoplasmosis and have been described in association with other diseases (intraocular lymphoma). However, they can help guide the diagnosis of OT and prevent the use of more invasive techniques, such as PCR analysis of vitreous fluid. The presence of residual cysts could be related to the pathogenesis of infection reactivations. The establishment of a standardised protocol for assessment with OCT and further studies on the subject could increase our understanding of OT.

References

1. Bonfioli AA, Orefice F. Toxoplasmosis. *Semin Ophthalmol.* 2007;20:129–41.
2. Garweg JG, de Groot-Mijnes JD, Montoya JG. Diagnostic approach to ocular toxoplasmosis. *Ocul Immunol Inflamm.* 2011;19: 255–61.
3. Harper TW, Miller D, Schiffman JC, Davis JL. Polymerase chain reaction analysis of aqueous and vitreous specimens in the diagnosis of posterior segment infectious uveitis. *Am J Ophthalmol.* 2009;147:140–7.
4. Yonekawa Y, Abbey AM, van Laere L, Shah AR, Thomas BJ, Ruby AJ, et al. Staghmite-like preretinal inflammatory deposits in vitrectomized eyes with posterior uveitis. *Digit J Ophthalmol.* 2017;23:18–22.
5. Ouyang Y, Pleyer U, Shao Q, Keane PA, Stübiger N, Jousseaume AM, et al. Evaluation of cystoid change phenotypes in ocular toxoplasmosis using optical coherence tomography. *PLoS One.* 2014;9:e86626.

Tessie Ferrer Mellor^{a,*}, Belén Sevilla Pérez^a,
Javier Lacorzana^b, Beatriz Bravo Mancheño^c,
Jose Luís García Serrano^d

^a Servicio de Pediatría, Hospital Universitario San Cecilio, Granada, Spain

^b Servicio de Oftalmología, Hospital Virgen de las Nieves, Granada, Spain

^c Servicio de Pediatría, Hospital Virgen de las Nieves, Granada, Spain

^d Servicio de Oftalmología, Hospital Universitario San Cecilio, Granada, Spain

* Corresponding author.

E-mail address: Tessieferrer90@gmail.com (T. Ferrer Mellor).

2 August 2018 10 October 2018

2341-2879/ © 2019 Asociación Española de Pediatría. Published by Elsevier España, S.L.U. This is an open access article under the CC BY-NC-ND license (<http://creativecommons.org/licenses/by-nc-nd/4.0/>).

Skin infiltration as a presenting sign of congenital leukaemia: presentation of two cases[☆]



Infiltración cutánea como manifestación de leucemia congénita: presentación de dos casos

To the Editor

Congenital leukaemia (CL) is defined as leukaemia with onset in the neonatal period, and accounts for fewer than 1 % of cases of infant leukaemia. Contrary to the pattern in the rest of childhood, two thirds of cases correspond to acute myeloid leukaemia (AML). It typically presents with cytopaenia, hyperleukocytosis, hepatosplenomegaly and coagulopathy and, in up to 60 % of patients, cutaneous infiltration.¹ This article presents 2 cases of CL managed in our hospital.

The first was an infant aged 2 months that had onset with fever and malaise. From the first month of life, the patient exhibited a purplish, elastic lump in the anterior fontanelle, with subsequent development of nodules in a generalised distribution. This was associated with pallor of the skin and mucosae, hepatosplenomegaly, respiratory failure and generalised hypertonia. The salient findings of blood tests were anaemia (4.4 g/dL), thrombocytopenia (66,000/mm³), leucocytosis (38,440/mm³) with atypia, elevation of lactate dehydrogenase (LDH) (2357 U/L) and hyperuricemia (7.49 mg/dL). The acute phase reactants were negative. The diagnosis of CD10-B-precursor acute lymphoblastic leukaemia (ALL) was confirmed by bone marrow aspiration. Fluorescence in situ hybridization (FISH) detected rearrangement of the *MLL* gene (11q23) with the t(10;11) translocation, and chromosome analysis revealed a normal 46 XX karyotype. The findings of cerebrospinal fluid (CSF) analysis, funduscopy and transfontanellar ultrasound examination were normal. The patient received chemotherapy following the Interfant-99 protocol for the high-risk group and achieved complete remission after the induction phase with persistence of *MLL*+. After completing the consolidation phase, the patient underwent a pretransplantation evaluation that revealed bone marrow infiltration with 80 %

of myeloid blasts (M0–M1), infiltration of the CSF and additional skin lesions. Molecular tests once again detected the t(10;11) translocation. Following cytoreductive chemotherapy (hydroxyurea, cytarabine and tioguanine), the patient was treated with intravenous fludarabine and intrathecal chemotherapy, achieving a second complete remission. Later on, the patient underwent haematopoietic stem cell transplantation (HSCT) of peripheral cord blood cells from a matched unrelated donor after conditioning with busulfan, cyclophosphamide, thiopeta and thymoglobulin. Full donor chimerism was not achieved and the patient experienced a second marrow relapse with a myeloid immune phenotype, which was treated with a FLAG-Ida regimen (idarubicin, fludarabine and cytarabine). The patient experienced recurrence of massive infiltration by lymphoid blasts during haematologic recovery, and died at age 12 months.

The second patient was an infant aged 7 weeks that developed indurated purplish nodular lesions in the skin with a generalised distribution starting at 20 days of age (Fig. 1), accompanied by pallor of the skin and mucosae and splenomegaly. The salient findings of blood tests were leucocytosis (32,910/mm³) with atypia, anaemia (8.7 g/dL), thrombocytopenia (100,000/mm³), elevation of LDH (661 U/L) and coagulopathy. Examination of a bone marrow aspiration sample revealed infiltration with 90 % of blasts with an immune phenotype compatible with M0 AML, and FISH revealed *MLL* rearrangement with no evidence of translocation. There was no central nervous system infiltration. The patient received chemotherapy following the St Jude AML 02 protocol, with resolution of the skin lesions on day 8 and complete full remission with a minimal residual disease of less than 0.1 % after the first cycle of ADE (cytarabine, etoposide, daunorubicin). After a second cycle of ADE, the patient, in first complete remission, underwent HSCT of $\alpha\beta$ /CD19-depleted peripheral blood from a haploidentical donor (the mother). The patient had achieved complete chimerism at 30 days post transplantation, and the only complication she experienced was grade 3 acute cutaneous graft versus host disease, which has since resolved. The patient is in complete remission 15 months after the diagnosis.

The incidence of CL is estimated at 1–5 cases per million live births. Approximately 65 % of cases are cases of AML compared to 35 % of cases of ALL.¹ Due to the immaturity of haematopoietic stem cells in these patients, co-expression of myeloid and lymphoid markers is frequent in the neonatal period, and so is lineage switch, as illustrated by the first case presented here. The diagnosis of CL also requires the presence of blasts in blood or bone marrow and extramedullary haematopoietic organs, ruling

[☆] Please cite this article as: Hernández MC, Catalán MA, Angulo BM, Robleda AC, López LM. Infiltración cutánea como manifestación de leucemia congénita: presentación de dos casos. *An Pediatr (Barc)*. 2020;92:106–108.